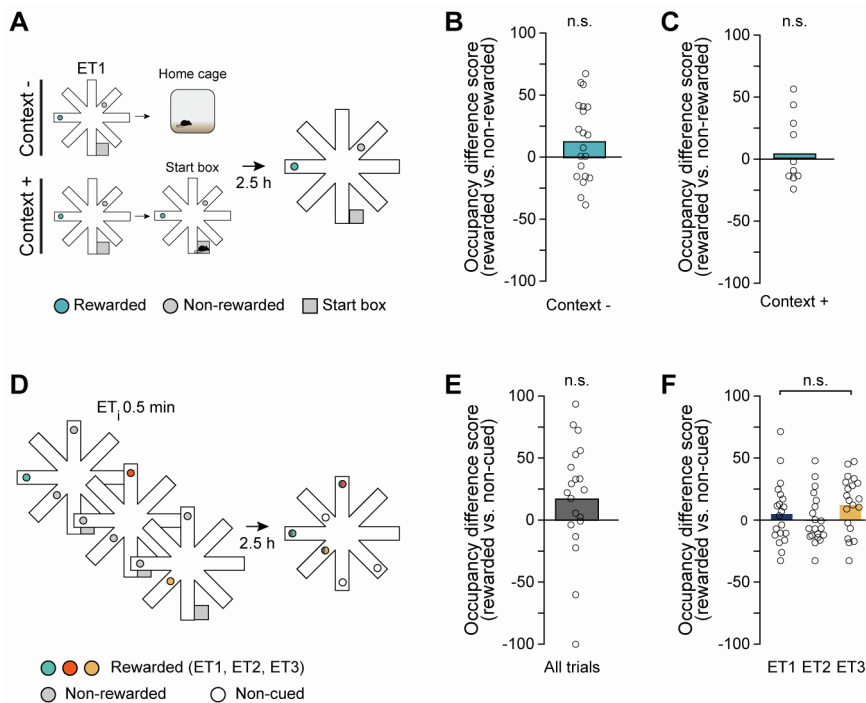


**Current Biology, Volume 31**

**Supplemental Information**

**Spaced training enhances memory  
and prefrontal ensemble stability in mice**

**Annet Glas, Mark Hübener, Tobias Bonhoeffer, and Pieter M. Goltstein**



**Figure S1. Only congruent, multi-trial training resulted in memory in the everyday memory task. Related to Figure 1.**

**(A)** Single trial learning experiment. A single encoding trial was conducted, after which the mouse was kept in the home cage during the entire retrieval delay (no re-introduction: Context -), or briefly re-introduced into the start box (Context +). After a retrieval delay of 2.5 h, a probe trial was conducted, and the occupancy at the rewarded and non-rewarded sandwell was recorded.

**(B)** Memory retrieval (occupancy difference) was not observed in the probe trial upon training with a single encoding trial without re-introduction (Wilcoxon signed-rank test: Context -,  $W = 126$ ,  $p = 0.078$ ,  $n = 20$  mice).

**(C)** Same as in **(B)** for a single encoding trial with re-introduction (Wilcoxon signed-rank test: Context +,  $W = 29$ ,  $p = 0.922$ ,  $n = 10$  mice).

**(D)** Incongruent learning experiment. Between ET1, ET2, and ET3 (encoding intertrial interval [ET<sub>i</sub>] 0.5 min), the location of the rewarded sandwell was altered. After a retrieval delay of 2.5 h, a probe trial was conducted.

**(E)** Occupancy was similar for previously rewarded sandwells and all non-cued sandwells (Wilcoxon signed-rank test: rewarded vs. non-cued sandwells,  $W = 155$ ,  $p = 0.062$ ,  $n = 20$  mice).

**(F)** Occupancy was similar for all of the previously rewarded sandwells (Friedman's ANOVA:  $\chi^2 = 2.03$ ,  $p = 0.363$ ,  $n = 20$  mice).

Circles indicate data from each mouse and bars indicate population mean. n.s., non-significant.

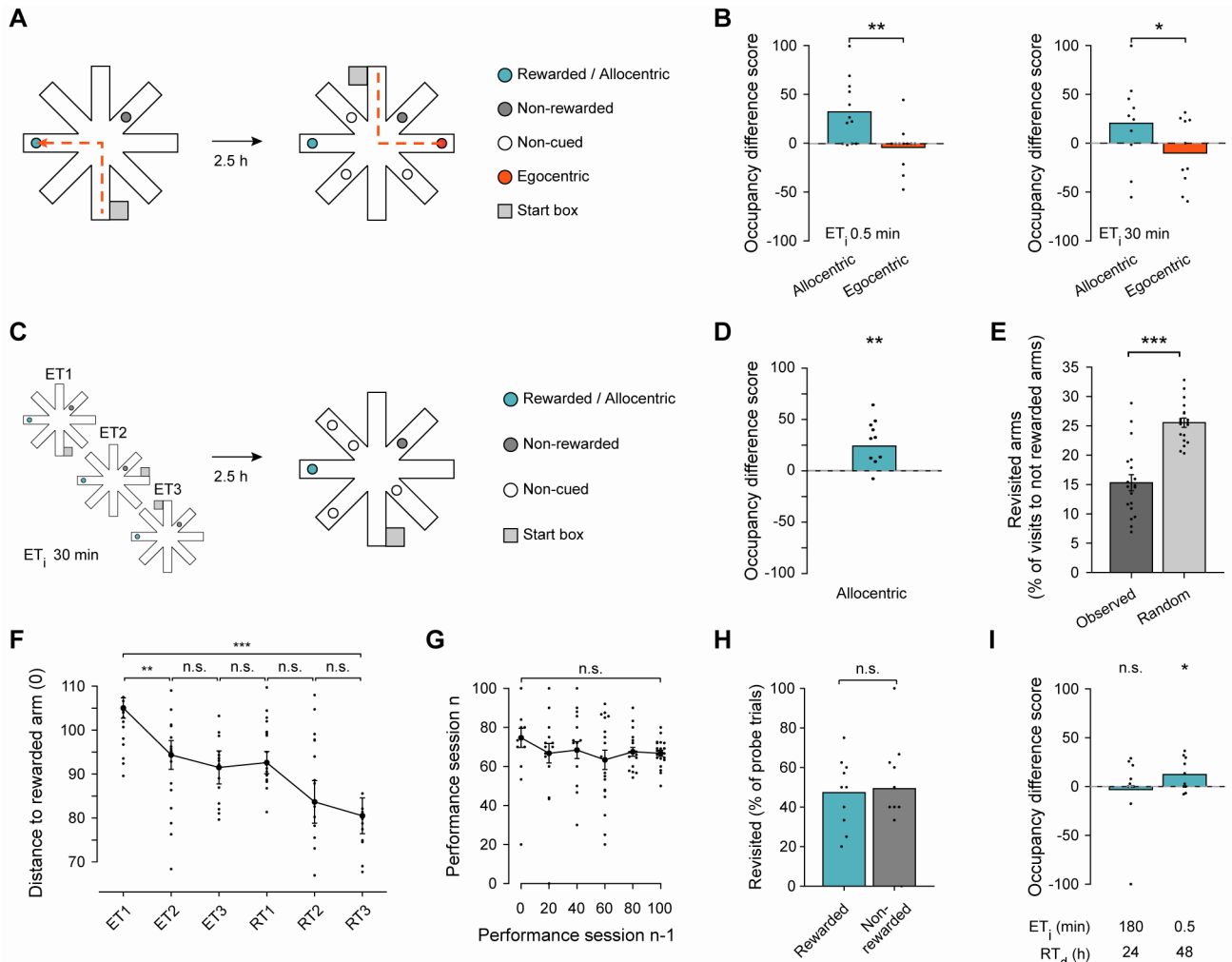


**Figure S2. Navigational strategies and extended delays in the everyday memory task. Related to Figure 1.**

**(A)** Navigational strategy experiment. Mice were trained on three encoding trials using either massed (ET<sub>i</sub> 0.5 min) or spaced (ET<sub>i</sub> 30 min) training. During the retrieval delay, the start box was placed at the opposite end of the maze, altering the path but not the location of the rewarded sandwell (“allocentric sandwell”). Egocentric spatial navigation would lead the mouse to a non-cued sandwell (“egocentric sandwell”).

**(B)** The occupancy at the allocentric versus egocentric sandwell upon both massed (left; paired-sample t-test:  $t_{11} = 3.69$ ,  $p = 3.59 \cdot 10^{-3}$ ,  $n = 12$  mice) and spaced training (right; paired-sample t-test:  $t_9 = 2.40$ ,  $p = 0.040$ ,  $n = 10$  mice).

**(C)** Forced allocentric strategy experiment. The start box location was altered after each encoding trial (ET<sub>i</sub> 30 min), enforcing allocentric navigation.

**(D)** Occupancy at the rewarded sandwell (one-sample t-test: observed vs. chance [occupancy difference 0],  $t_9 = 3.50$ ,  $p = 0.007$ ,  $n = 10$  mice).

**(E)** The observed, relative fraction of incorrect arm visits was lower than expected from chance (paired-sample t-test: observed vs. random arm visits,  $t_{18} = -13.5$ ,  $p = 7.50 \cdot 10^{-11}$ ,  $n = 19$  mice).

**(F)** The mean angular distance of the arm the mouse was in, relative to the rewarded arm (OWRM ANOVA:  $F_{5,90} = 8.17$ ,  $p = 3.00 \cdot 10^{-6}$ , Bonferroni post hoc tests for subsequent trials: ET<sub>1</sub> vs. ET<sub>2</sub>,  $p = 1.17 \cdot 10^{-3}$ ,  $n = 19$  mice).

**(G)** The performance in RT<sub>1</sub> of the previous session did not affect that of the current session (OWRM ANOVA:  $F_{5,90} = 0.61$ ,  $p = 0.695$ ,  $n = 19$  mice).

**(H)** In probe trials in which the mouse entered and subsequently left the rewarded or non-rewarded arm, revisiting the respective arm did not depend on whether it previously contained a reward (paired-sample t-test: revisiting rewarded vs. non-rewarded arm,  $t_9 = -0.33$ ,  $p = 0.748$ ,  $n = 10$  mice).

**(I)** Occupancy at the rewarded sandwell upon training with an extended encoding intertrial interval (one-sample t-test: ET<sub>i</sub> 180 min, RT<sub>d</sub> 24 h observed vs. chance [occupancy difference 0],  $t_9 = -0.26$ ,  $p = 0.799$ ,  $n = 10$  mice) or an extended retrieval delay (one-sample t-test: ET<sub>i</sub> 0.5 min, RT<sub>d</sub> 48 h observed vs. chance [occupancy difference 0],  $t_9 = 2.31$ ,  $p = 0.046$ ,  $n = 10$  mice).

Dots indicate data from each mouse, circles and bars indicate the population mean, errorbars indicate SEM. n.s., non-significant, \*  $p < 0.05$ , \*\*  $p < 0.01$ , \*\*\*  $p < 0.001$ .

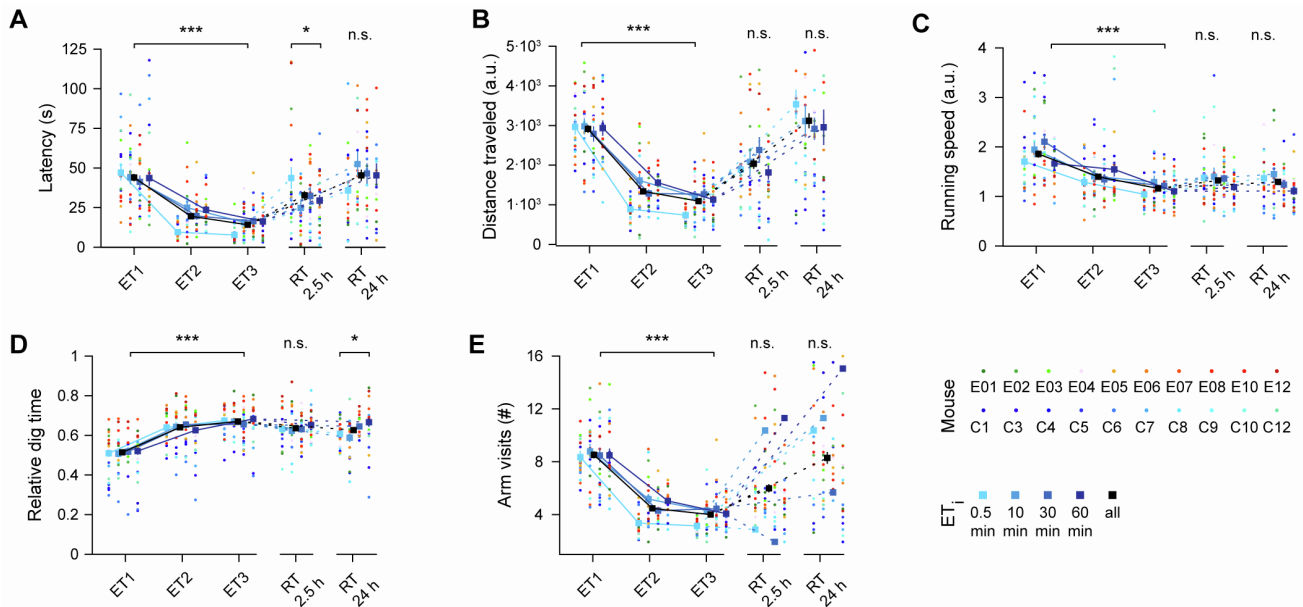


**Figure S3. Behavioral parameters of individual mice in the everyday memory task. Related to Figure 1.**

The mean values of individual mice ( $n = 19$ ) are represented by colored dots and are sorted by the session's  $ET_i$  (0.5, 10, 30, or 60 min). The means for each trial, pooled across mice and  $ET_i$ s, are represented by black lines and squares.

**(A)** Latency to the rewarded arm in  $ET_1$ ,  $ET_2$ , and  $ET_3$  (“consecutive encoding trials”: TWRM ANOVA: encoding trial identity [ETID],  $F_{2,108} = 71.5$ ,  $p = 6.58 \cdot 10^{-13}$ ;  $ET_i$ ,  $F_{3,108} = 1.93$ ,  $p = 0.137$ ; Bonferroni post hoc test:  $ET_1$  vs.  $ET_2$ ,  $p = 2.00 \cdot 10^{-6}$ ;  $ET_1$  vs.  $ET_3$ ,  $p = 1.10 \cdot 10^{-7}$ ;  $ET_2$  vs.  $ET_3$ ,  $p = 1.14 \cdot 10^{-3}$ ;  $n = 19$  mice) and the first retrieval trial ( $RT_1$ ) after a retrieval delay ( $RT_d$ ) of 2.5 h (OWRM ANOVA:  $F_{3,54} = 3.76$ ,  $p = 0.016$ ,  $n = 19$  mice) or 24 h (OWRM ANOVA:  $F_{3,54} = 1.16$ ,  $p = 0.334$ ,  $n = 19$  mice).

**(B)** Same as in **(A)**, for the distance traveled (TWRM ANOVA: consecutive encoding trials: ETID,  $F_{2,108} = 174$ ,  $p = 1.29 \cdot 10^{-18}$ ;  $ET_i$ ,  $F_{3,108} = 3.08$ ,  $p = 0.036$ ; Bonferroni post hoc test:  $ET_1$  vs.  $ET_2$ ,  $p = 8.63 \cdot 10^{-10}$ ;  $ET_1$  vs.  $ET_3$ ,  $p = 1.11 \cdot 10^{-10}$ ;  $ET_2$  vs.  $ET_3$ ,  $p = 0.003$ ; OWRM ANOVA:  $RT_d$  2.5 h,  $F_{3,54} = 1.51$ ,  $p = 0.224$ ;  $RT_d$  24 h,  $F_{3,54} = 0.564$ ,  $p = 0.641$ ,  $n = 19$  mice).

**(C)** Same as in **(A)**, for the running speed (TWRM ANOVA: consecutive encoding trials: ETID,  $F_{2,108} = 27.9$ ,  $p = 6.88 \cdot 10^{-8}$ ;  $ET_i$ ,  $F_{3,108} = 2.60$ ,  $p = 0.063$ ; Bonferroni post hoc test:  $ET_1$  vs.  $ET_2$ ,  $p = 0.002$ ;  $ET_1$  vs.  $ET_3$ ,  $p = 9.00 \cdot 10^{-6}$ ;  $ET_2$  vs.  $ET_3$ ,  $p = 0.007$ ; OWRM ANOVA:  $RT_d$  2.5 h,  $F_{3,54} = 0.98$ ,  $p = 0.410$ ;  $RT_d$  24 h,  $F_{3,54} = 2.49$ ,  $p = 0.074$ ,  $n = 19$  mice).

**(D)** Same as in **(A)**, for the relative dig time (TWRM ANOVA: consecutive encoding trials: ETID,  $F_{2,108} = 73.2$ ,  $p = 4.80 \cdot 10^{-13}$ ;  $ET_i$ ,  $F_{3,108} = 1.04$ ,  $p = 0.384$ ; Bonferroni post hoc test:  $ET_1$  vs.  $ET_2$ ,  $p = 1.37 \cdot 10^{-6}$ ;  $ET_1$  vs.  $ET_3$ ,  $p = 4.04 \cdot 10^{-8}$ ; OWRM ANOVA:  $RT_d$  2.5 h,  $F_{3,54} = 0.91$ ,  $p = 0.445$ ;  $RT_d$  24 h,  $F_{3,54} = 3.42$ ,  $p = 0.024$ ,  $n = 19$  mice).

**(E)** Same as in **(A)**, for the number of arm visits (TWRM ANOVA: consecutive encoding trials: ETID,  $F_{2,108} = 133$ ,  $p = 7.80 \cdot 10^{-17}$ ;  $ET_i$ ,  $F_{3,108} = 3.84$ ,  $p = 0.015$ ; Bonferroni post hoc test:  $ET_1$  vs.  $ET_2$ ,  $p = 4.44 \cdot 10^{-9}$ ;  $ET_1$  vs.  $ET_3$ ,  $p = 8.85 \cdot 10^{-10}$ ; OWRM ANOVA:  $RT_d$  2.5 h,  $F_{3,54} = 1.59$ ,  $p = 0.204$ ;  $RT_d$  24 h,  $F_{3,54} = 1.03$ ,  $p = 0.386$ ,  $n = 19$  mice).

Squares and bars indicate mean  $\pm$  SEM across animals. n.s., non-significant, \*  $p < 0.05$ , \*\*\*  $p < 0.001$ .

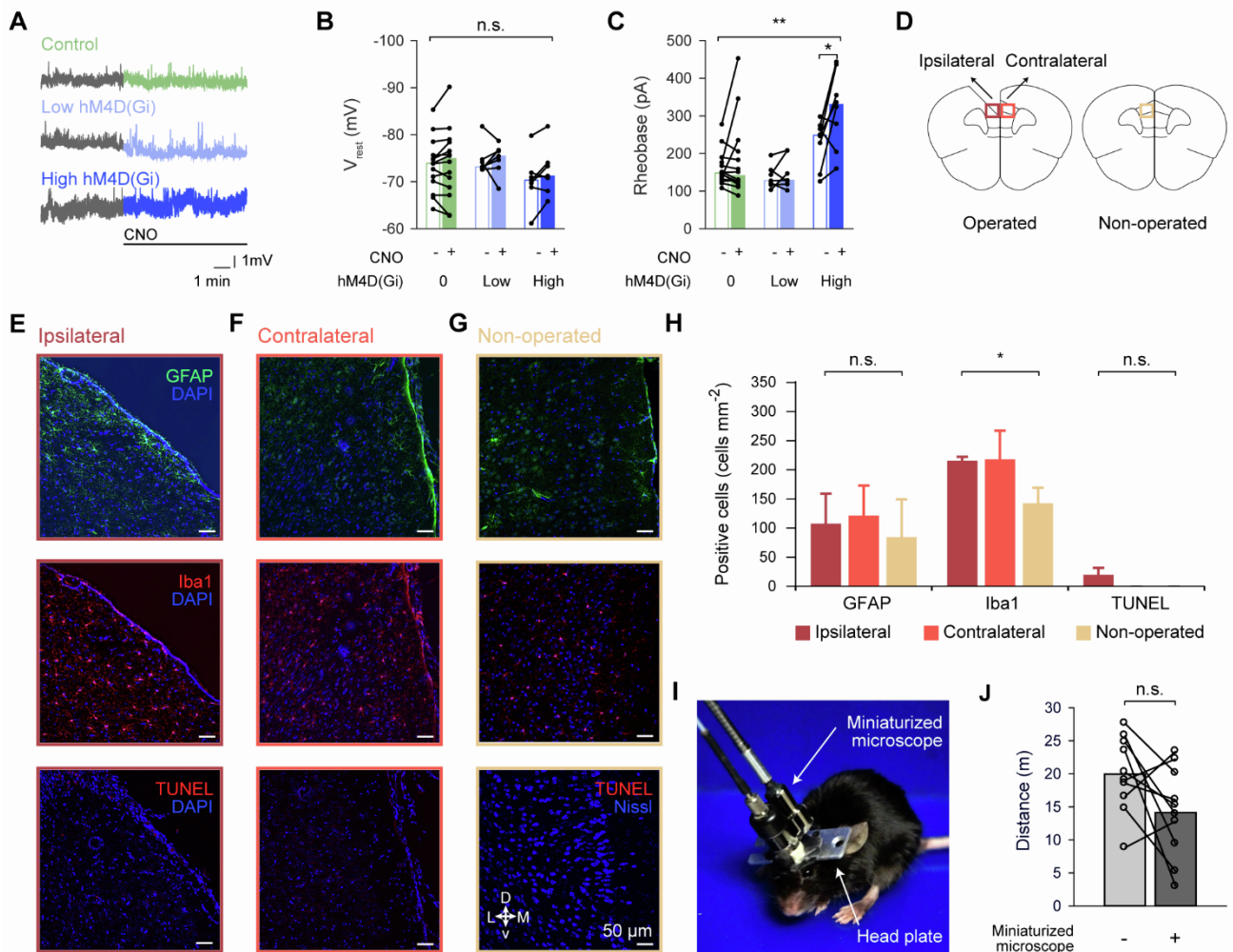


**Figure S4. Control experiments regarding chemogenetic inactivation and miniaturized microscope imaging of the dmPFC. Related to Figures 3 and 4.**

(A) Example *ex vivo* current-clamp recordings of the membrane potential of neurons not transduced (control;  $n = 14$  neurons), transduced with a low titer (titer  $2.3 \cdot 10^{10}$  GC  $\text{ml}^{-1}$ ;  $n = 7$  neurons), or transduced with a high titer (titer  $2.3 \cdot 10^{12}$  GC  $\text{ml}^{-1}$ ;  $n = 7$  neurons) hM4D(Gi)-encoding AAV before and after clozapine-*N*-oxide (CNO) application.

(B) CNO application did not affect the resting membrane potential ( $V_{\text{rest}}$ ; TWRM ANOVA: CNO,  $F_{1,25} = 2.38$ ,  $p = 0.135$ ,  $n = 28$  neurons).

(C) CNO application affected rheobase (TWRM ANOVA: CNO,  $F_{1,25} = 8.16$ ,  $p = 0.008$ ,  $n = 28$  neurons), post hoc analysis revealed an effect for high hM4D(Gi)-expressing neurons (paired-sample *t*-test:  $t_6 = -2.62$ ,  $p = 0.034$ ,  $n = 7$  neurons).

(D) A subsection of the ipsilateral and contralateral dmPFC hemisphere of mice with (operated) or without (non-operated) a microprism implant was analyzed for markers of astrogliosis (GFAP expression), microgliosis (Iba1 expression) and apoptosis (TUNEL assay).

(E–G) Representative intensity adjusted micrographs of dmPFC sections from the ipsilateral hemisphere (E), contralateral hemisphere (F), and non-operated hemisphere (G) labeled with GFAP (top), Iba1 (middle), and TUNEL (bottom).

(H) The number of GFAP-expressing (Kruskal-Wallis test:  $H_2 = 0.35$ ,  $p = 0.840$ ), Iba1-expressing (Kruskal-Wallis test:  $H_2 = 6.05$ ,  $p = 0.049$ ), and TUNEL-positive (Kruskal-Wallis test:  $H_2 = 3.85$ ,  $p = 0.146$ ) cells in the ipsilateral and contralateral ( $n = 4$  mice) and non-operated ( $n = 3$  mice) hemispheres.

(I) Mouse carrying a miniaturized microscope, mounted on a head plate implant.

(J) The distance mice traveled was not significantly affected by carrying the miniaturized microscope (paired-sample *t*-test: - vs. +,  $t_9 = 1.92$ ,  $p = 0.084$ ,  $n = 10$  mice).

Recordings from individual neurons (filled circles) are connected with lines, bars indicate population means, open circles indicate data from one mouse. Scale bars 50  $\mu\text{m}$  (E–G). n.s., non-significant, \*  $p < 0.05$ , \*\*  $p < 0.01$ .

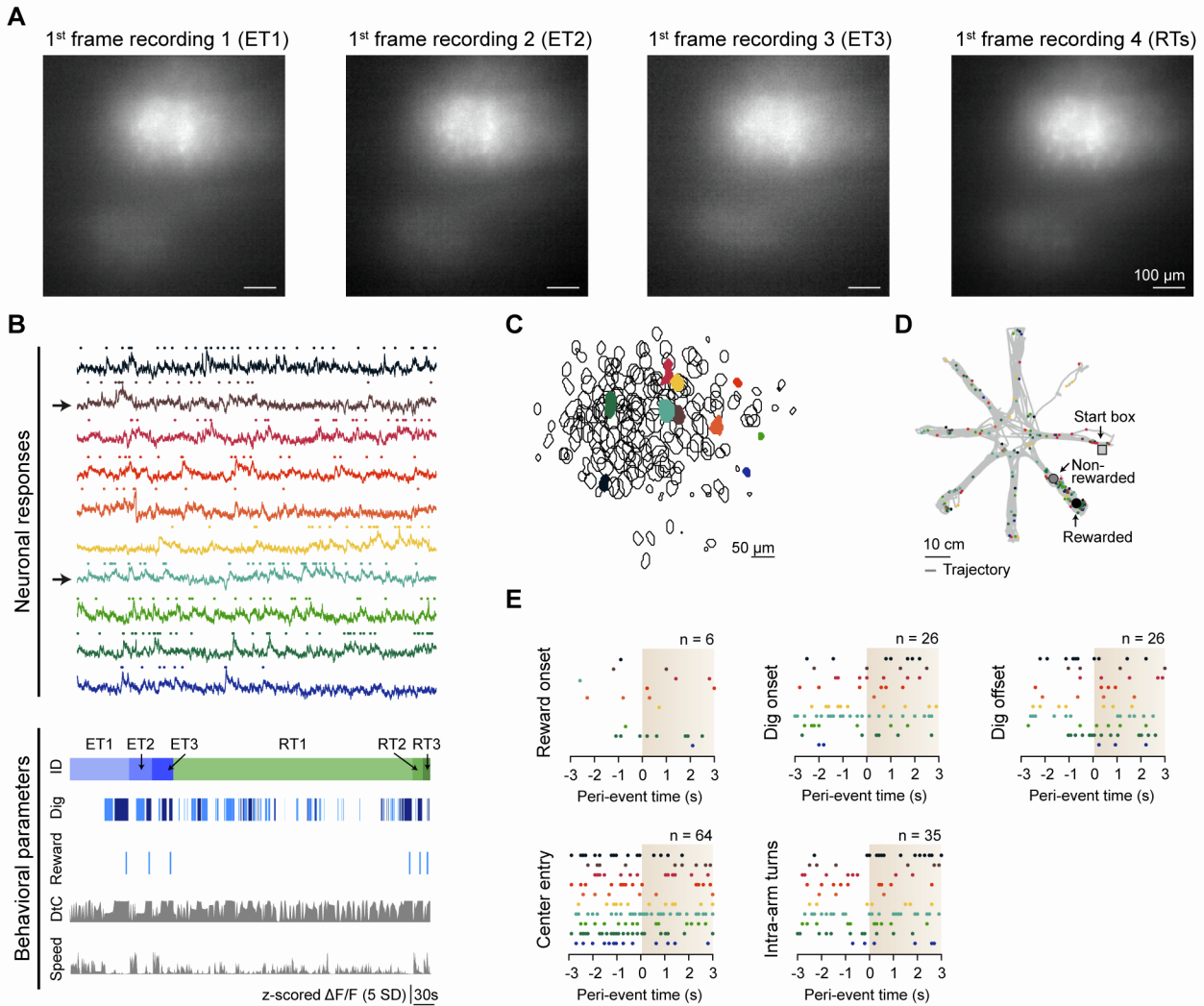


**Figure S5. *In vivo* calcium imaging of dmPFC neuronal populations in the everyday memory task. Related to Figures 4 and 6.**

(A) Realigned first microscopy frames from the first, second, third, and fourth recording of an example behavioral session in which the miniature microscope was removed and replaced in-between trials. Across sessions, the 95<sup>th</sup> percentile of the field of view shift was 6 pixels.

(B) Responses of 10 example neurons (top) and behavioral parameters (bottom) during an example session. Two partially overlapping sources are indicated with an arrow. Behavioral parameters include digging at the rewarded (dark blue) and non-rewarded sandwell (blue), reward consumption (“Reward”), distance to center (“DtC”; max-normalized distance to the central platform), and running speed of the mouse (“Speed”).

(C) Outlines of all neurons (black lines) in the field of view of the miniaturized microscope. Example neurons are indicated by color.

(D) Locations where the example neurons fired along the mouse’s trajectory from the start box via various arms to the non-rewarded sandwell and rewarded sandwell.

(E) Peri-event responses of the example neurons, aligned to reward onset (n = 6 events), digging onset (n = 26 events), digging offset (n = 6 events), entry into the center platform (n = 64 events), and intra-arm turns (n = 35 events).

Filled dots indicate spikes, color-coded by neuron identity. ID: trial identity SD: standard deviation. Scale bars: 100  $\mu\text{m}$  (A), 30 s (B), 50  $\mu\text{m}$  (C), 10 cm (D).



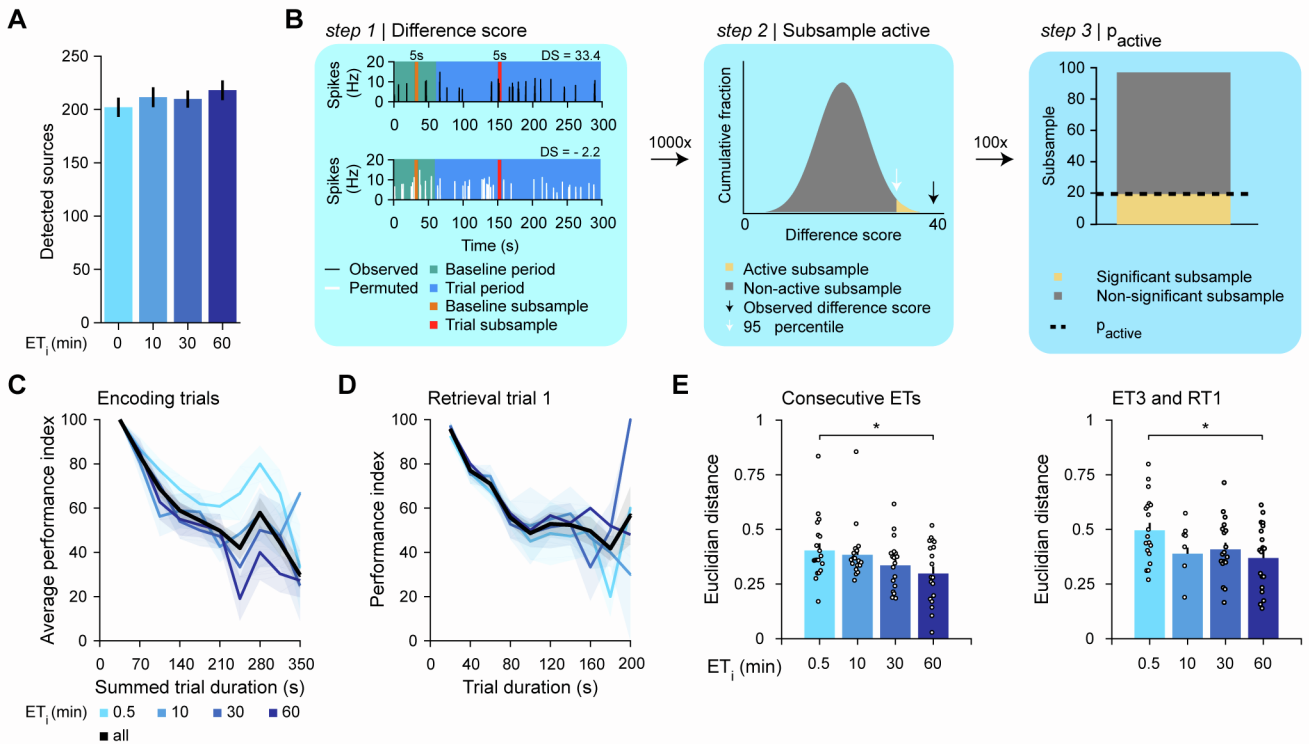


**Figure S6. Quantification of the activity and stability of a neuronal population. Related to Figure 4.**

**(A)** The number of sources detected by the CNMF-E algorithm, sorted by ET<sub>i</sub> (OWRM ANOVA:  $F_{3,54} = 2.09$ ,  $p = 0.113$ ,  $n = 19$  mice).

**(B)** Approach to quantify neural activity ( $p_{\text{active}}$ ) within a trial. Step 1: quantify difference score (DS) for 5-second subsample of inferred spiking activity. Step 2: permutation of spike trace, re-quantify DS. The neuron was qualified as active in this subsample when observed DS > 95<sup>th</sup> percentile of permuted DSs. Step 3: repeat steps 1 and 2 100 times with different baseline and trial subsamples. The sum of active subsamples, divided by 100, yielded the  $p_{\text{active}}$  for this neuron in this trial.

**(C)** The behavioral performance on, and duration of, all encoding trials of a session, sorted by ET<sub>i</sub>. Across all sessions, encoding trial duration correlated significantly with performance (Spearman correlation:  $r_s = -0.40$ ,  $p = 1.02 \cdot 10^{-20}$ ,  $n = 499$  sessions).

**(D)** As in **(C)**, but for the first retrieval trial of a session (Spearman correlation:  $r_s = -0.49$ ,  $p = 6.59 \cdot 10^{-32}$ ,  $n = 499$  sessions).

**(E)** Euclidian distance of the ensemble response vectors, sorted by ET<sub>i</sub>, between consecutive encoding trials (ET1, ET2, and ET3) and between ET3 and RT1 (OWRM ANOVA: consecutive ETs: ET<sub>i</sub>,  $F_{3,54} = 3.71$ ,  $p = 0.017$ ; ET3-RT1: ET<sub>i</sub>,  $F_{3,54} = 5.97$ ,  $p = 0.001$ , Bonferroni post hoc tests: 0.5 vs. 10 min,  $p = 0.009$ ; 0.5 vs. 30 min,  $p = 0.017$ ; 0.5 vs. 60 min,  $p = 0.011$ ,  $n = 19$  mice).

Circled dots indicate data from individual mice, bars and error bars indicate population mean and SEM, lines and shaded area indicate mean and SEM, respectively. n.s., non-significant, \*  $p < 0.05$ .